Crystal structure of lubiprostone Polymorph B, $C_{20}H_{32}F_2O_5$

James A. Kaduk,[1,2,a] Amy M. Gindhart,[3] and Thomas N. Blanton[3]
[1]*Illinois Institute of Technology, 3101 S. Dearborn St., Chicago, Illinois 60616*
[2]*North Central College, 30 N. Brainard St., Naperville, Illinois 60540*
[3]*ICDD, 12 Campus Blvd., Newtown Square, Pennsylvania 19073-3273*

(Received 26 May 2018; accepted 17 July 2018)

The crystal structure of lubiprostone has been refined using synchrotron X-ray powder diffraction data, and optimized using density functional techniques. Lubiprostone crystallizes in space group *P*1 (#1) with $a = 9.02025(2)$, $b = 10.72121(2)$, $c = 12.32817(4)$ Å, $\alpha = 78.5566(2)$, $\beta = 69.6858(2)$, $\gamma = 77.3292(2)°$, $V = 1081.069(3)$ Å^3, and $Z = 2$. The two independent molecules occur in an extended conformation, aligned approximately along the *c*-axis. The hydrophobic side chains are adjacent to each other, resulting in layers parallel to the *ac* plane. The two carboxylic acid groups form an eight-membered ring, resulting in dimers of the two independent molecules. Each hydroxyl group acts as a hydrogen bond donor to the ketone of the fused ring system. The powder pattern is included in the Powder Diffraction File™ as entry 00-066-1622. © *2018 International Centre for Diffraction Data*. [doi:10.1017/S0885715618000660]

Key words: lubiprostone, powder diffraction, Rietveld refinement, density functional theory

I. INTRODUCTION

Lubiprostone (brand name AMITIZA®) is used in the management of chronic idiopathic constipation, predominantly irritable bowel syndrome-associated constipation in women and opiod-induced constipation. Lubiprostone is a chloride channel activator and functions by increasing the amount of fluid in the intestine making stool passage easier. The systematic name (CAS Registry number 136790-76-6) is 7-[(1R,3R,6R,7R)-3-(1,1-difluoropentyl)-3-hydroxy-8-oxo-2-oxabicyclo[4.3.0]non-7-yl]heptanoic acid. A two-dimensional molecular diagram of lubiprostone is shown in Figure 1.

X-ray powder diffraction patterns of Polymorphs A and B of lubiprostone are reported in US Patent 8 513 441 (Alberico *et al*., 2013; Alphora Research Inc., Mississauga, Ontario, Canada). The pattern of another polymorph, designated APO-II, is reported in US Patent 8 785 663 (Ceccarelli and Kothakonda, 2014; Apotex Pharmachem Inc., Brantford, Ontario, Canada).

This work was carried out as part of a project (Kaduk *et al*., 2014) to determine the crystal structures of large-volume commercial pharmaceuticals, and include high-quality powder diffraction data for them in the Powder Diffraction File (Fawcett *et al*., 2017).

II. EXPERIMENTAL

Lubiprostone was a commercial regent, purchased from Sigma-Aldrich (Batch No. 124M4704 V), and was used as-received. The white powder was packed into a 1.5 mm diameter Kapton capillary, and rotated during the measurement at ~50 cycles s^{-1}. The powder pattern was measured at 295 K at beam line 11-BM (Lee *et al*., 2008; Wang *et al*., 2008) of the Advanced Photon Source at Argonne National Laboratory using a wavelength of 0.414163 Å from 0.5–50° 2θ with a step size of 0.001° and a counting time of 0.1 s step^{-1}. The pattern was indexed on a primitive triclinic unit cell with $a = 9.0174$, $b = 10.7188$, $c = 12.3300$ Å, $\alpha = 78.563$, $\beta = 69.684$, $\gamma = 77.312°$, $V = 1080.5$ Å^3, and $Z = 2$ using Jade (MDI, 2016) and N-TREOR (Altomare *et al*., 2013). Since lubiprostone is a chiral molecule, the space group was

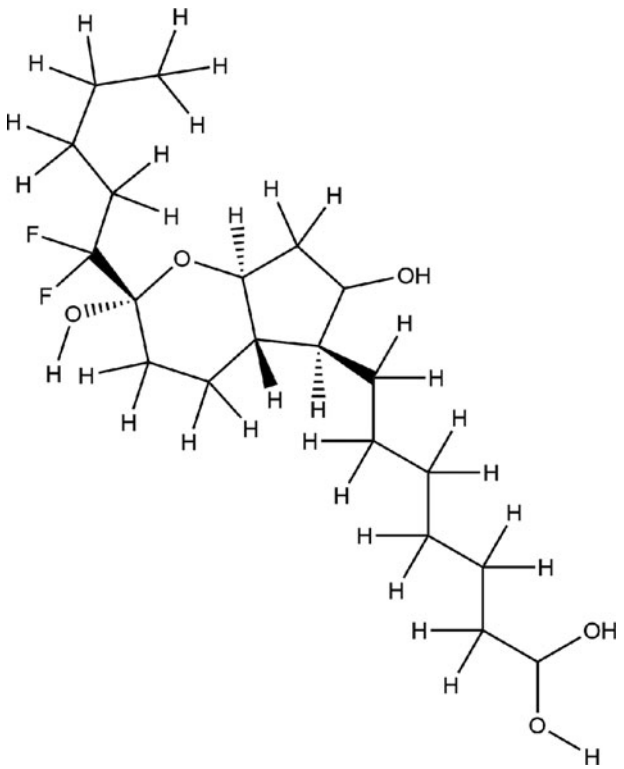

Figure 1. The molecular structure of lubiprostone.

[a]Author to whom correspondence should be addressed. Electronic mail: kaduk@polycrystallography.com

assumed to be *P*1. A reduced cell search in the Cambridge Structural Database (Groom *et al*., 2016) combined with the chemistry "C H F O only" yielded no hits.

A lubiprostone molecule was built using Spartan '16 (Wavefunction Inc., 2017), and its equilibrium conformation determined using molecular mechanics techniques. The resulting .mol2 file was converted into a Fenske–Hall *Z*-matrix file using OpenBabel (O'Boyle *et al*., 2011). Attempts to solve the structure using FOX (Favre-Nicolin and Černý, 2002) and DASH (David *et al*., 2006) were unsuccessful. During the structure solution, a Grant-in-Aid submission which became PDF entry 00-065-1086 for lubiprostone (Peng, 2014) arrived at ICDD Headquarters, with coordinates of the non-hydrogen atoms derived from an unpublished single-crystal study. The coordinates of the hydrogen atoms were computed in Materials Studio (Dassault, 2014) and manually by assessing potential hydrogen bonding.

Rietveld refinement was carried out using GSAS (Toby, 2001; Larson and Von Dreele, 2004). Only the 2.0–22.0° portion of the pattern was included in the refinement (d_{min} = 1.085 Å). All non-H bond distances and angles were subjected to restraints, based on a Mercury/Mogul Geometry Check (Bruno *et al*., 2004; Sykes *et al*., 2011) of the molecule. The Mogul average and standard deviation for each quantity were used as the restraint parameters. The restraints contributed 12.7% to the final χ^2. The displacement coefficients in the two independent molecules were constrained to be the same. A common U_{iso} was refined for the non-H atoms of the ring system, another U_{iso} for the two hydroxy oxygen atoms, another U_{iso} for the non-H atoms of the F-containing side chains, and another U_{iso} for the non-H atoms of the carboxylic acid side chains. The U_{iso} of each hydrogen atom was fixed at 1.3× that of the heavy atom to which it was attached. The peak profiles were described using profile function #4 (Thompson *et al*., 1987; Finger *et al*., 1994), which includes the Stephens (1999) anisotropic strain broadening model. The background was modeled using a three-term shifted Chebyshev polynomial, with a three-term diffuse-scattering function to model the Kapton capillary and any amorphous component. The final refinement of 200 variables using 20136 observations (20000 data points and 136 restraints) yielded the residuals R_{wp} = 0.0891, R_p = 0.0725, and χ^2 = 2.989. The largest peak (0.76 Å from C38 and hole (1.51 Å from O13) in the difference Fourier map were 0.43 and −0.50 eÅ^{-3}, respectively. The Rietveld plot is included as Figure 2. The largest errors in the fit are in the shapes and positions of some of the low-angle peaks, and may reflect changes in the specimen during the measurement.

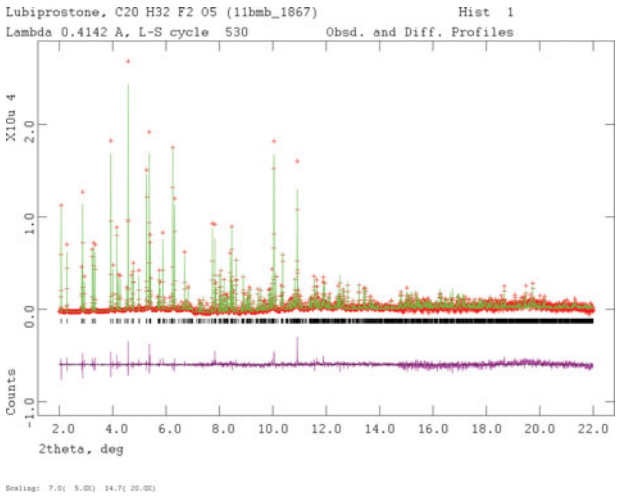

Figure 2. (Color online) The Rietveld plot for the refinement of lubiprostone. The red crosses represent the observed data points, and the green line is the calculated pattern. The magenta curve is the difference pattern, plotted at the same vertical scale as the other patterns. The vertical scale has been multiplied by a factor of 5 for $2\theta > 7.0$, and by a factor of 20 for $2\theta > 14.7$.

A density functional geometry optimization (fixed experimental unit cell) was carried out using CRYSTAL14 (Dovesi *et al*., 2014). The basis sets for H, C, and O were those of Gatti *et al*. (1994), that for F was from Peintinger *et al*. (2013). The calculation was run on eight 2.1 GHz Xeon cores (each with 6 Gb RAM) of a 304-core Dell Linux cluster at IIT, used 8 *k*-points and the B3LYP functional, and took ∼4.3 days.

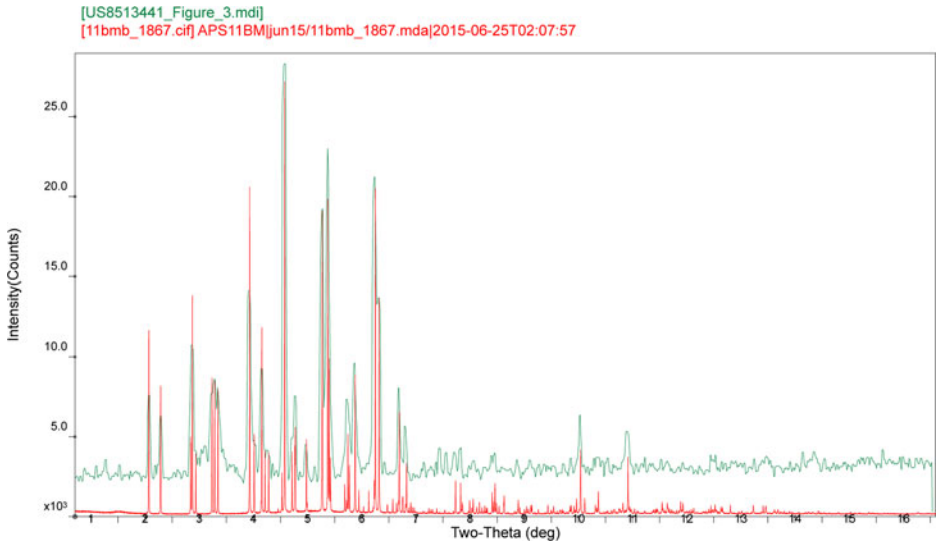

Figure 3. (Color online) Comparison of the powder pattern of lubiprostone to the pattern of Figure 3 of US Patent 8 513 441 for the Polymorph B of lubiprostone claimed by Alphora Research Inc.

https://doi.org/10.1017/S0885715618000660 Published online by Cambridge University Press

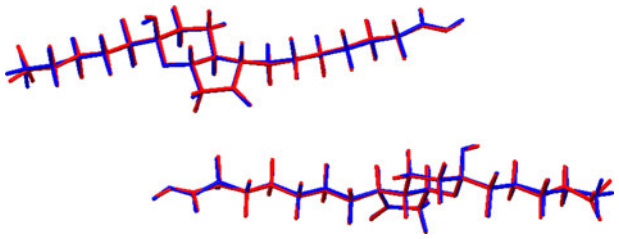

Figure 4. (Color online) Comparison of the refined and optimized structures of lubiprostone. The Rietveld refined structure is in red, and the DFT-optimized structure is in blue.

III. RESULTS AND DISCUSSION

The observed powder pattern is similar enough to Figure 3 of US Patent 8 513 441 [Figure 3, digitized using UN-SCAN-IT 7.0 (Silk Scientific, 2013)] to conclude that this sample is Polymorph B of lubiprostone. The refined atom coordinates of lubiprostone and the coordinates from the DFT optimization are reported in the CIFs attached as Supplementary Material. The root-mean-square deviation of the non-hydrogen atoms is only 0.10 Å (Figure 4). The excellent agreement between the refined and optimized structures is evidence that the experimental structure is correct (van de Streek and Neumann, 2014). This discussion uses the DFT-optimized structure. The asymmetric unit (with atom numbering) is illustrated in Figure 5, and the crystal structure is presented in Figure 6.

Almost all of the bond distances, bond angles, and torsion angles in lubiprostone fall within the normal ranges indicated by a Mercury Mogul Geometry check (Macrae *et al.*, 2008). The F3-C39-C40 angle [optimized = 106.3°, average = 109.1 (8)°, *Z*-score = 3.46] is flagged as unusual, the result of the exceptionally low uncertainty on the average. The torsion angles C23-C24-C28-C29 and C43-C44-C48-C49 are *trans* rather than the more-normal *gauche*, and the torsion angles C25-C24-C28-C29 and C45-C44-C48-C49 are *gauche* instead of the normal *trans*.

The two independent lubiprostone molecules have a similar extended conformation. The root-mean-square Cartesian displacement is 0.409 Å. The largest difference is in the conformations of the carboxyl groups. The molecules are aligned roughly along the *c*-axis. The hydrophobic side chains lie adjacent to each other. The result is layers of molecules parallel to the *ac* plane.

Quantum chemical geometry optimizations (Hartree–Fock/6-31G*/water) using Spartan '16 (Wavefunction Inc., 2017) indicated that the two independent molecules are within 0.5 kcal mole^{-1} of each other in energy. The two molecules converge to the same local minimum. A molecular mechanics conformational analysis indicated that the observed solid-state conformation is 19.6 kcal mol^{-1} higher in energy than global minimum energy conformation of an isolated molecule. In the minimum-energy conformation, the carboxylic acid side chain curls up to form a hydrogen bond to the ketone of the fused ring system. The difference shows that both hydrogen bonding and interchain interactions are important in determining the solid-state conformation.

Analysis of the contributions to the total crystal energy using the Forcite module of Materials Studio (Dassault, 2014) suggests that bond angle distortion terms are the most significant contributions to the intramolecular deformation energy, but that bond distance and torsion terms also contribute. The intermolecular energy is dominated by van der Waals attractions and electrostatic repulsions, which in this force-field-based analysis include hydrogen bonds. The hydrogen bonds are better analyzed using the results of the DFT calculation.

The two carboxylic acid groups form a ring with graph set (Etter, 1990; Bernstein *et al.*, 1995; Shields *et al.*, 2000) *R*2,2 (8), resulting in a dimer of the two independent molecules (Table I). Each of the hydroxyl groups acts as a hydrogen bond donor to a ketone of the fused ring system. These discrete hydrogen bonds link the molecules along the *b*-axis. The energies of these O–H···O hydrogen bonds were calculated from the Mulliken overlap populations according to the correlation of Rammohan and Kaduk (2018).

The Bravais–Friedel–Donnay–Harker (Bravais, 1866; Friedel, 1907; Donnay and Harker, 1937) morphology suggests that we might expect blocky morphology for

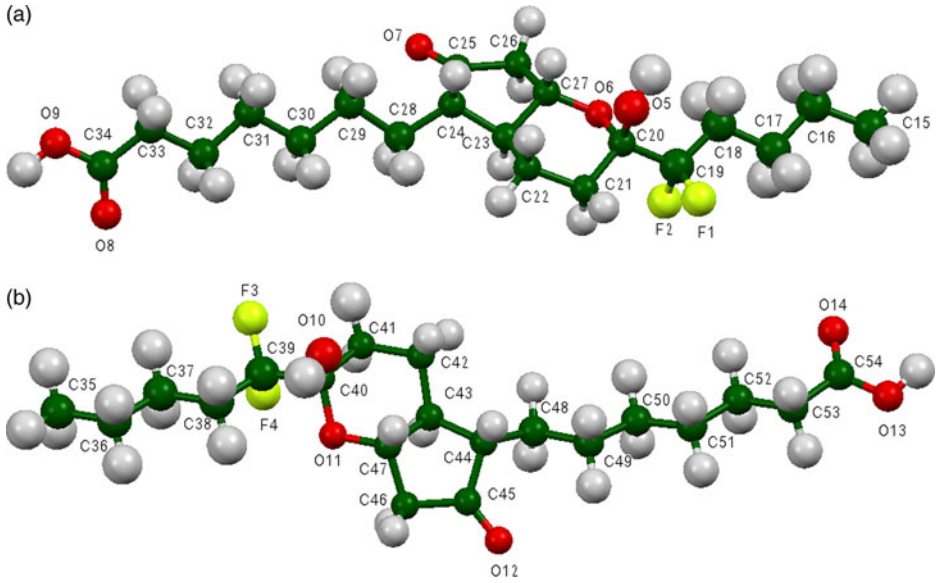

Figure 5. (Color online) The refined molecular structures of the two independent lubiprostone molecules, with the atom numbering. The atoms are represented by 50% probability spheroids. (*a*) Molecule 1. (*b*) Molecule 2.

https://doi.org/10.1017/S0885715618000660 Published online by Cambridge University Press

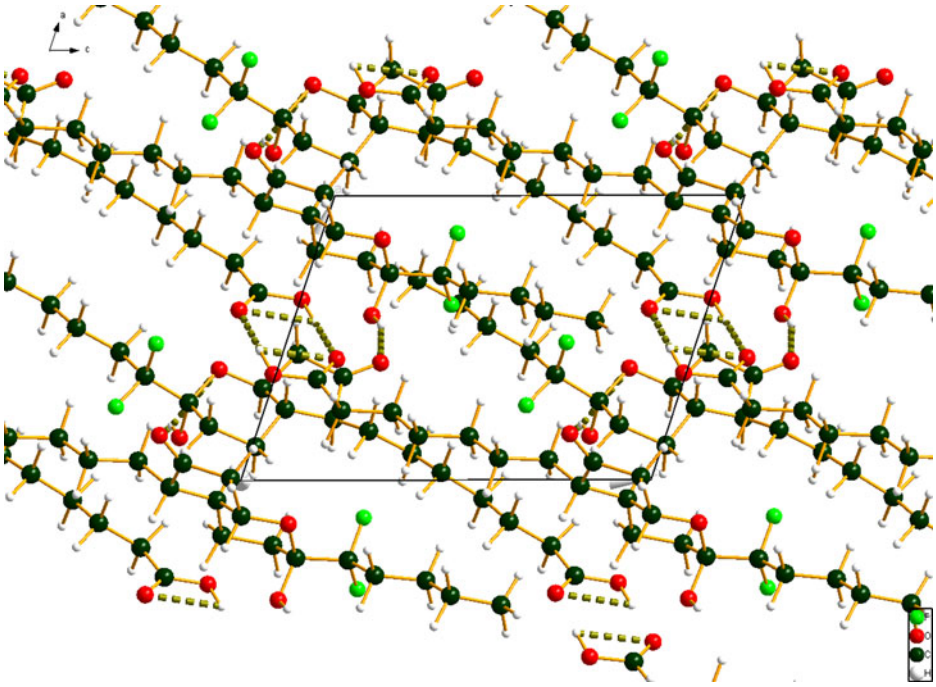

Figure 6. (Color online) The crystal structure of lubiprostone, viewed down the *b*-axis.

TABLE I. Hydrogen bonds (CRYSTAL14) in lubiprostone.

H-bond	D–H, Å	H···A, Å	D···A, Å	D–H···A,°	Overlap, *e*	Energy, kcal mol^{-1}
O9–H56···O14	1.008	1.637	2.644	178.0	0.074	14.9
O13–H58···O8	1.007	1.609	2.615	177.0	0.070	14.5
O5–H55···O12	0.981	1.815	2.725	152.8	0.054	12.7
O10–H57···O10	0.981	1.822	2.720	150.6	0.052	12.5

lubiprostone, with {001}, {010}, and {100} as principal faces. A second-order spherical harmonic preferred orientation model was included in the refinement; the texture index was only 1.0004, indicating that preferred orientation was not significant in this rotated capillary specimen. The powder pattern of lubiprostone is included in the Powder Diffraction File™ as entry 00-066-1622.

SUPPLEMENTARY MATERIAL

The supplementary material for this article can be found at https://doi.org/10.1017/S0885715618000660.

ACKNOWLEDGEMENTS

Use of the Advanced Photon Source at Argonne National Laboratory was supported by the US Department of Energy, Office of Science, Office of Basic Energy Sciences, under Contract No. DE-AC02-06CH11357. This work was partially supported by the International Centre for Diffraction Data. The authors thank Lynn Ribaud for his assistance in data collection, and Andrey Rogachev for the use of computing resources at IIT.

Alberico, D., Clayton, J., Gorin, B. I., and Oudenes, J. (**2013**). "Prostaglandin synthesis and intermediates for use therein," US Patent 8 513 441.

Altomare, A., Cuocci, C., Giacovazzo, C., Moliterni, A., Rizzi, R., Corriero, N., and Falcicchio, A. (**2013**). "EXPO2013: a kit of tools for phasing crystal structures from powder data," J. Appl. Crystallogr. **46**, 1231–1235.

Bernstein, J., Davis, R. E., Shimoni, L., and Chang, N. L. (**1995**). "Patterns in hydrogen bonding: functionality and graph set analysis in crystals," Angew. Chem. Int. Ed. English **34**, 1555–1573.

Bravais, A. (**1866**). *Etudes Cristallographiques* (Gauthier Villars, Paris).

Bruno, I. J., Cole, J. C., Kessler, M., Luo, J., Motherwell, W. D. S., Purkis, L. H., Smith, B. R., Taylor, R., Cooper, R. I., Harris, S. E., and Orpen, A. G. (**2004**). "Retrieval of crystallographically-derived molecular geometry information," J. Chem. Inf. Sci. **44**, 2133–2144.

Ceccarelli, A. P. and Kothakonda, K. K. (**2014**). "Polymorphic forms of lubiprostone," US Patent 8 785 663.

Dassault Systèmes (**2014**). *Materials Studio 8.0* (BIOVIA, San Diego, CA).

David, W. I. F., Shankland, K., van de Streek, J., Pidcock, E., Motherwell, W. D. S., and Cole, J. C. (**2006**). "DASH: a program for crystal structure determination from powder diffraction data," J. Appl. Crystallogr. **39**, 910–915.

Donnay, J. D. H. and Harker, D. (**1937**). "A new law of crystal morphology extending the law of Bravais," Am. Mineral. **22**, 446–467.

Dovesi, R., Orlando, R., Erba, A., Zicovich-Wilson, C. M., Civalleri, B., Casassa, S., Maschio, L., Ferrabone, M., De La Pierre, M., D-Arco, P., Noël, Y., Causà, M., and Kirtman, B. (**2014**). "CRYSTAL14: a program for the ab initio investigation of crystalline solids," Int. J. Quantum Chem. **114**, 1287–1317.

Etter, M. C. (**1990**). "Encoding and decoding hydrogen-bond patterns of organic compounds," Acc. Chem. Res. **23**, 120–126.

Favre-Nicolin, V. and Černý, R. (**2002**). FOX, "free objects for crystallography: a modular approach to ab initio structure determination from powder diffraction," J. Appl. Crystallogr. **35**, 734–743.

Fawcett, T. G., Kabekkodu, S. N., Blanton, J. R., and Blanton, T. N. (**2017**). "Chemical analysis by diffraction: the Powder Diffraction File™," Powder Diffr. **32**, 63–71.

Finger, L. W., Cox, D. E., and Jephcoat, A. P. (**1994**). "A correction for powder diffraction peak asymmetry due to axial divergence," J. Appl. Crystallogr. **27**, 892–900.

Friedel, G. (**1907**). "Etudes sur la loi de Bravais," Bull. Soc. Fr. Mineral. **30**, 326–455.

Gatti, C., Saunders, V. R., and Roetti, C. (**1994**). "Crystal-field effects on the topological properties of the electron-density in molecular crystals – the case of urea," J. Chem. Phys. **101**, 10686–10696.

Groom, C. R., Bruno, I. J., Lightfoot, M. P., and Ward, S. C. (**2016**). "The Cambridge Structural Database," Acta Crystallogr. Sect. B Struct. Sci. Cryst. Eng. Mater. **72**, 171–179.

Kaduk, J. A., Crowder, C. E., Zhong, K., Fawcett, T. G., and Suchomel, M. R. (**2014**). "Crystal structure of atomoxetine hydrochloride (Strattera), $C_{17}H_{22}NOCl$," Powder Diffr. **29**, 269–273.

Larson, A. C. and Von Dreele, R. B. (**2004**). *General Structure Analysis System, (GSAS)*, (Los Alamos National Laboratory Report LAUR 86–784).

Lee, P. L., Shu, D., Ramanathan, M., Preissner, C., Wang, J., Beno, M. A., Von Dreele, R. B., Ribaud, L., Kurtz, C., Antao, S. M., Jiao, X., and Toby, B. H. (**2008**). "A twelve-analyzer detector system for high-resolution powder diffraction," J. Synchroton. Radiat. **15**, 427–432.

Macrae, C. F., Bruno, I. J., Chisholm, J. A., Edington, P. R., McCabe, P., Pidcock, E., Rodriguez-Monge, L., Taylor, R., van de Streek, J., and Wood, P. A. (**2008**). "Mercury CSD 2.0 – new features for the visualization and investigation of crystal structures," J. Appl. Crystallogr. **41**, 466–470.

MDI (**2016**). *Jade 9.7* (Materials Data. Inc., Livermore, CA).

O'Boyle, N., Banck, M., James, C. A., Morley, C., Vandermeersch, T, and Hutchison, G. R. (**2011**). "Open Babel: an open chemical toolbox," J. Chem. Informatics **3**, 33.

Peintinger, M. F., Vilela Oliveira, D., and Bredow, T. (**2013**). "Consistent Gaussian basis sets of triple-zeta valence with polarization quality for solid-state calculations," J. Comput. Chem. **34**, 451–459.

Peng, Y. (**2014**). Powder Diffraction File entry 00-065-1086. ICDD Grant-in-Aid, Tianjin Institute of X-ray Analysis, Nankai District, P. R. China.

Rammohan, A. and Kaduk, J. A. (**2018**). "Crystal structures of alkali metal (Group 1) citrate salts", Acta Cryst. Sect. B: Cryst. Eng. Mater. **74**, 239–252.

Shields, G. P., Raithby, P. R., Allen, F. H., and Motherwell, W. S. (**2000**). "The assignment and validation of metal oxidation states in the Cambridge Structural Database," Acta Crystallogr. Sect. B Struct. Sci. **56**, 455–465.

Silk Scientific (**2013**). *UN-SCAN-IT 7.0* (Silk Scientific Corporation, Orem, UT).

Stephens, P. W. (**1999**). "Phenomenological model of anisotropic peak broadening in powder diffraction," J. Appl. Crystallogr. **32**, 281–289.

Sykes, R. A., McCabe, P., Allen, F. H., Battle, G. M., Bruno, I. J., and Wood, P. A. (**2011**). "New software for statistical analysis of Cambridge Structural Database data," J. Appl. Crystallogr. **44**, 882–886.

Thompson, P., Cox, D. E., and Hastings, J. B. (**1987**). "Rietveld refinement of Debye-Scherrer synchrotron X-ray data from Al_2O_3," J. Appl. Crystallogr. **20**, 79–83.

Toby, B. H. (**2001**). "EXPGUI, a graphical user interface for GSAS," J. Appl. Crystallogr. **34**, 210–213.

van de Streek, J. and Neumann, M. A. (**2014**). "Validation of molecular crystal structures from powder diffraction data with dispersion-corrected density functional theory (DFT-D)," Acta Crystallogr. Sect. B Struct. Sci. Cryst. Eng. Mater. **70**, 1020–1032.

Wang, J., Toby, B. H., Lee, P. L., Ribaud, L., Antao, S. M., Kurtz, C., Ramanathan, M., Von Dreele, R. B., and Beno, M. A. (**2008**). "A dedicated powder diffraction beamline at the Advanced Photon Source: commissioning and early operational results," Rev. Sci. Inst. **79**, 085105.

Wavefunction, Inc. (**2017**). Spartan '16 Version 2.0.3, Wavefunction Inc., 18401 Von Karman Ave., Suite 370, Irvine CA 92612.